47th AIAA Aerospace Sciences Meeting Including The New Horizons Forum and Aerospace Exposition
5 - 8 January 2009, Orlando, Florida

AIAA 2009-1419

Swirl Effects on Mixing in Free Underexpanded Supersonic-Nozzle Airflow

A. Abdelhafez,[*] A. Kareem,[†] and A. K. Gupta[‡]
Department of Mechanical Engineering, University of Maryland
College Park, MD 20742

This study complements our previous experimental investigation of the effects of swirl, convective Mach number, and air-fuel density ratio on shock structure in non-swirling and swirling underexpanded airflows with coaxial fuel injection. The effects of the above parameters on mixing are investigated experimentally in this present work. A novel nanosecond condensate-seeded Mie-scattering diagnostic technique was used to highlight the variation of mixedness within the flowfield. It was found that swirl enhances mixing significantly and reduces the strength of shock structure, which agrees with the findings of previous research. Higher convective Mach numbers allow for near-complete mixing of fuel jet with the surrounding airflow, as the interactions of shock structure with air/fuel shear layer are sufficient to achieve complete mixing. This behavior disappears steadily as convective Mach number is reduced. The shear angle between fuel and air jets was found to depend on fuel compressibility and air-fuel density ratio. Incompressible fuel jets and/or high air-fuel density ratios result in negative shear angles, which transition to positive if the fuel jet becomes compressible or the density gradient across shear layer decreases. If this density gradient approaches unity, the Baroclinic vorticity loses strength, which results in deteriorated mixing.

Nomenclature

a	=	speed of sound
DR	=	air-fuel density ratio
M	=	Mach number
M_{conv}	=	convective Mach number
p	=	pressure
R	=	specific gas constant
T	=	absolute temperature
t	=	time
v	=	velocity
ρ	=	density
γ	=	ratio of specific heats
$\vec{\omega}_{bc}$	=	Baroclinic vorticity vector

I. Introduction

Although hypersonic vehicles, powered by supersonic airbreathing engines, are the future of high-speed flight, some critical science issues pertinent to supersonic combustion have not been fully understood yet. These issues include mixing and ignition in scramjet engines. It is desired to maintain supersonic flow through a scramjet combustor, in order to avoid the losses in total pressure and temperature inherent in decelerating the hypersonic incoming flow to subsonic speeds. Successful operation of any air-breathing vehicle depends on efficient mixing, ignition, and combustion.[1] The efficiency and effectiveness of an injection system are defined by the achievable degree of fuel/air mixing and the system capability of minimizing injection-induced thrust losses, respectively.[2] Supersonic flows are compressible and resistant to fuel penetration and mixing. Therefore, the equivalence ratio of scramjet-engine operation has to be fuel-rich over a considerable part of the vehicle flight, in order to ensure that a flame is present to provide positive thrust. Any progress made on improving the engine efficiency must, therefore, be closely followed towards achieving efficient mixing between fuel and air. Scramjet flows have residence times of the order of only few milliseconds. In this short residence time, one must account for the mixing, ignition delay, and combustion time scales.

To shed some light on this technical challenge, Figure 1 shows a simplified chemical-kinetics analysis, similar to the one conducted in Abdelhafez and Gupta.[3] Plotted are the chronological variations of temperature and Mach number for H_2/air mixtures of different equivalence ratios inside a plug-flow constant-area reactor. Fuel-rich conditions are considered, as is the case in actual scramjet operation. Perfect mixing and injection are assumed, i.e., hydrogen mixes with air instantaneously, homogeneously, and loss-free over the entire reactor cross-section after injection. The inlet air temperature and Mach number are chosen to be 1000 K and 4.0, respectively, as common representatives of conditions after the inlet and isolator sections of a hypersonic vehicle. The assumption of loss-free injection allows for considering a constant H_2/air mixture temperature of 1000 K (independent of equivalence ratio) prior to ignition. Engine unstart is assumed not to occur, even at

[*] Graduate Student, Student Member AIAA
[†] Undergraduate Student
[‡] Distinguished University Professor, Fellow AIAA, akgupta@umd.edu

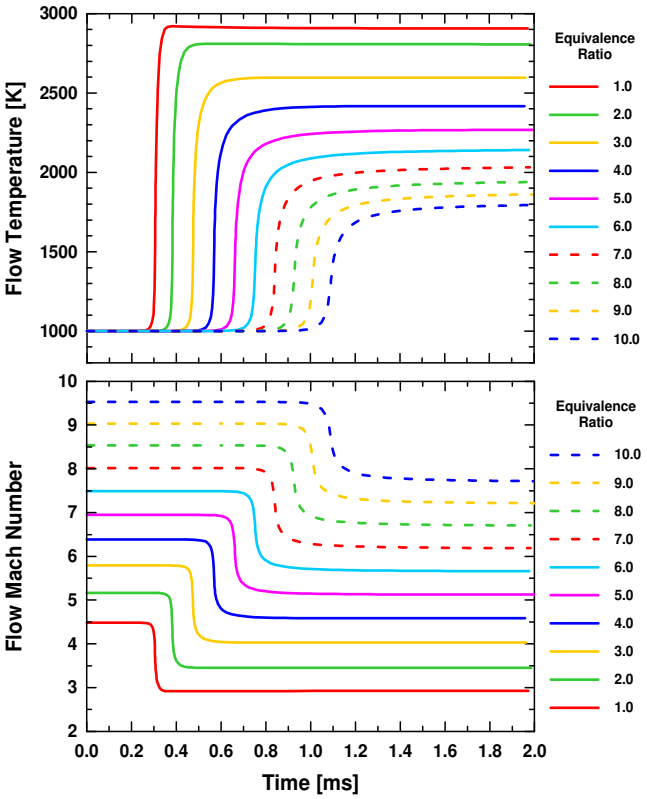

Figure 1. Evolution of flow temperature (top) and Mach number (bottom) in an adiabatic, perfectly-stirred, plug-flow, constant-area H_2/air reactor at different equivalence ratios of operation. Initial air Mach number and temperature = 4.0 and 1000 K, respectively

extremely high equivalence ratios. The design shock-on-lip inlet condition is assumed to be fulfilled at all times. Consequently, the same air flow rate is captured, regardless of equivalence ratio. The latter is thus controlled through fuel flow rate. In an attempt to reduce ignition delay, adiabatic conditions are assumed, i.e. the combustor walls are not cooled, as the actual operating conditions dictate. The Chemkin Pro 4.5 code was used with the standard built-in GRI chemical-kinetics mechanism of hydrocarbon reactions.

It can be seen from Figure 1 that the ignition delay increases from 0.25 to 1.0 ms with increase in equivalence ratio, which agrees well with the average value given in previous research.[4,5] The ignition delay is defined here as the time at which the step-like increase in temperature commences. It can be seen that the ignition-delay time scale under fuel-rich operating conditions is still considerably large, even with the assumption of adiabatic conditions. If, in addition to this challenge, wall cooling is incorporated, radical quenching must be accounted for. It can also be observed from the temperature distributions that higher equivalence ratios result in lower flow temperatures after combustion completion, due to the distribution of released chemical energy over higher flow rates of combustion products and unburned fuel. This reduction in post-combustion flow temperature has a negative effect on thrust development in vehicle nozzle downstream of combustor.

The evolution of flow Mach number in Figure 1 confirms the large magnitude of ignition-delay time scale. Higher Mach numbers are observed at higher equivalence ratios. However, it should be noted that this is an artifact of the ideal inlet and injection assumptions. Since it is assumed that a constant air flow rate is captured, higher equivalence ratios implicate higher flow rates of air-fuel mixture through the combustor. These higher flow rates translate into higher Mach numbers under loss-free injection assumptions. Such behavior would never exist in an actual scramjet engine, where fuel injection is accompanied by shock formation, which results in total-pressure and Mach-number losses. Moreover, engine unstart can occur at extreme equivalence ratios, if combustor static pressure becomes too high due to excessive shock formation.

While the temporal variations in flow Mach number appear qualitatively similar in Figure 1, some small yet important differences are revealed from Figure 2, where the inlet-to-exit reduction in Mach number (i.e., $M_i - M_e$) is plotted against equivalence ratio. This reduction represents losses due to the irreversible combustion of fuel and air. It can be clearly observed that increasing the equivalence ratio (up to about 6) results in higher loss of flow Mach number, which is one more disadvantage of fuel-rich operating conditions. Similar to the reduction in post-combustion flow temperature, the loss of Mach number has a detrimental effect on thrust production. A different trend is observed at equivalence ratios higher than 6. The reduction in Mach number becomes less severe, i.e., the ratio M_e/M_i increases slightly with equivalence ratio. This behavior can be explained through following analysis. From the basic definitions of Mach number, velocity, and density,

$$M = v/\sqrt{\gamma R T} \qquad v = \dot{m}/(\rho A) \qquad \rho = p/(RT)$$

one can write

$$M = \frac{\dot{m}}{\rho A}\cdot\frac{1}{\sqrt{\gamma R T}} = \frac{\dot{m}}{A}\cdot\frac{RT}{p}\cdot\frac{1}{\sqrt{\gamma}}\cdot\frac{1}{\sqrt{RT}}$$

$$\Rightarrow \quad M = \frac{\dot{m}}{A}\cdot\frac{\sqrt{RT}}{p\sqrt{\gamma}}$$

$$\Rightarrow \quad \frac{M_e}{M_i} = \left(\frac{p_i}{p_e}\right)\left(\frac{\gamma_i}{\gamma_e}\right)^{0.5}\left(\frac{R_e}{R_i}\right)^{0.5}\left(\frac{T_e}{T_i}\right)^{0.5}$$

Note that the flow rate and reactor cross-sectional area are constant for each equivalence ratio and thus cancel out. The ratios on right-hand side are plotted versus equivalence ratio in Figure 2. It can be observed that the changes in (γ_i/γ_e) and (R_i/R_e) are insignificant. At equivalence ratios up to 6 the decreasing (T_e/T_i) dominates, thus resulting in higher losses in Mach number. However, as the equivalence ratio of 6 is approached, the contradicting effects of (p_i/p_e) and (T_e/T_i) become comparable, which results in an almost constant

ratio (M_e/M_i). Minor recovery is observed beyond equivalence ratio of 6, as the effect of pressure ratio slowly overrides that of temperature ratio. It should be finally noted that the value of equivalence ratio beyond which recovery commences (6 in this case), depends on inlet conditions (i.e., T_i, p_i, and M_i) as well as fuel type.

In light of this analysis it can be seen how challenging the actual scramjet-engine operating conditions are, especially if a target residence time of few milliseconds is to be met. The situation becomes even more challenging, if the mixing time scale, mixture non-homogeneity, and injection losses are factored into the analysis. Failure to meet such strict demands reflects on the engine length, which, in turn, affects the vehicle weight, available payload, developed thrust, and specific impulse. Therefore, any progress made on improving engine efficiency must be closely followed towards achieving efficient mixing between fuel and air.

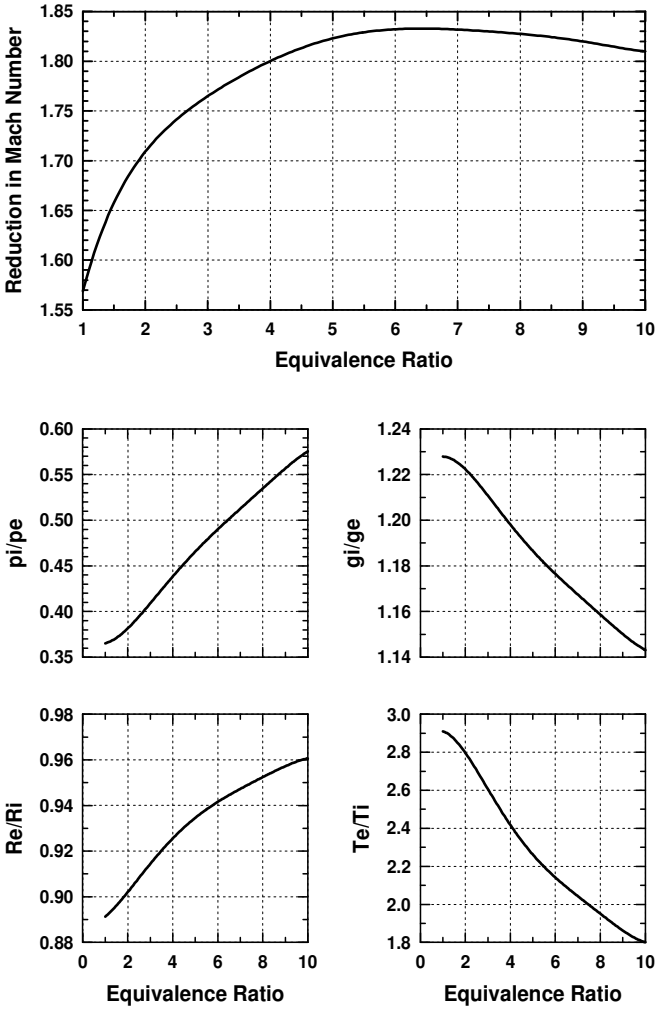

Figure 2. Variation of Mach-number reduction and other inlet-exit property ratios with equivalence ratio

Previous research has shown that flame holding in reacting supersonic flows is achieved by creating high-vorticity regions, where fuel and air partially mix at lower velocities.[6] In an experimental study Huh and Driscoll[7] successfully stabilized a supersonic H_2/air flame, with coaxial injection, along the axis of a Mach-2.5 wind tunnel. Stabilization was achieved by using small-angled wedges mounted on the tunnel sidewalls to generate weak oblique shock waves that interact with the flame. It was found that these shock waves enhance fuel-air mixing to the extent that the flame length decreased by up to 30% for certain shock locations and strengths, which are optimum for the investigated geometry and operating conditions. The researchers reasoned that the enhanced mixing is partially attributed to radial inflows of air induced by the shocks into the fuel jet. It was concluded that optimizing the mixing and stability limits for any combustor geometry requires careful matching of shock strengths and locations of shock/flame interaction.

Yang et al.[8] simulated shock-induced mixing numerically. Parallel flows of a heavy gas interspersed with other flows of a lighter one were overtaken by a normal shock wave. It was shown that vorticity is generated at each location of interaction of the density gradient across each light/heavy interface with the shock wave pressure gradient. Since the pressure and density gradient vectors are out of phase at these locations, their cross-product ($\nabla p \times \nabla \rho$) has non-zero values. This cross-product defines the Baroclinic vorticity vector, $\partial_t \vec{\omega}_{bc} = (\nabla p \times \nabla \rho)/\rho^2$, which causes the light gas regions to roll up into one or more counter-rotating vortex pairs, stirring and mixing the light and heavy gases together. It was concluded that, whenever possible, multiple shock waves should be utilized.

Shock waves of supersonic flows have significant positive effects on fuel-air mixing and flame stabilization, when they interact appropriately with the air/fuel shear layer. Some beneficial effects of this interaction are:[9] (a) directing the airflow locally towards fuel for increased entrainment rates, (b) creation of additional vorticity that enhances mixing, and (c) increasing the flow static pressure and temperature through a shock wave. The exact role of each effect needs further substantiation and quantification.

Research on subsonic swirling flows is abundant in the literature; however, little of a fundamental nature is known about supersonic swirling ones. The structure of highly under-expanded nozzle jets was investigated experimentally and analytically by Adamson and Nicholls[10]. They presented a method for calculating the position of the first Mach disc. In their calculation for a sonic orifice, the axial pressure distribution on flow centerline behind the orifice (calculated by method of characteristics) was used to define a fictitious nozzle extension. The shock was then assumed to exist at the point where atmospheric pressure would be attained behind the shock, i.e., the shock was assumed to exist at the end of fictitious nozzle extension. Physical arguments were

employed to extend the analysis to nozzles with supersonic exit Mach numbers. An approximate method for computing the jet boundary, up to the point of maximum jet area, was also given. The analytical results compared favorably with experimental data at relatively low nozzle pressure ratios.

In a relevant experimental investigation Crist et al.[11] studied the structure of underexpanded jets with stagnation pressures up to 15,000 psia, ambient pressures down to 100 μHg, and stagnation temperatures up to 4200 K. The location of Mach disk was found to be insensitive to the ratio of specific heats, nozzle-lip geometry, and absolute pressure. For over-all pressure ratios up to about 300,000 the location of Mach disk was found to vary as the square root of over-all pressure ratio. The diameters of Mach disk, jet boundary, and intercepting shock were found to increase with decrease in specific-heat ratio and to decrease at high stagnation density, where intermolecular forces become important. At high-pressure ratios, the ratio of Mach-disk diameter to Mach-disk position appeared to be constant for a given gas. It was also found that the properties along jet axis can be approximated by the properties of a flow through a hypothetical conical nozzle whose half-angle is given as a function of specific heat ratio. A simplified expression for the distribution of Mach number along the jet axis was given to good approximation as a function of specific-heat ratio.

Lewis and Carlson[12] experimentally determined the distance from nozzle exit plane to the first Mach disc in gas-only and gas-particle jets issuing from underexpanded supersonic nozzles. An empirical correlation of the data was presented which is valid for both jet types and incorporates the effect of gas specific-heat ratio.

Gostintsev et al.[13] studied an underexpanded supersonic swirling gas jet issuing from a convergent nozzle. They showed that the effect of rotation on the wave structure of axisymmetric jet is qualitatively analogous to the effect of reduction in overpressure ratio. Using formulas for spiral isentropic flow, an approximate expression was obtained for estimating the location of first Mach disc in the swirling flow downstream of nozzle exit.

Lewellen et al.[14] developed an approximation that can be used to determine how swirl affects the choking constraint on flow through the throat of a nozzle. It was found that the choking constraint imposes a limit on the maximum tangential Mach number that can be achieved in a vortex tube, even when an infinite pressure ratio is available. Moreover, analytic expressions were derived for the variation of rocket mass flow in a spinning rocket.

Batson and Sforzini[15] studied the structure of swirling flow through a convergent nozzle with emphasis on the effect of swirl on flowfield, thrust, and mass flow produced by nozzled devices, such as jet engines and spin-stabilized rockets. It was reported that the axial velocity component increases, whereas the tangential one decreases, after the flow transitions to supersonic through nozzle throat.

Naumova and Shmyglevskii[16] demonstrated with a simple example that avoidance of flow rotation is a limitation which might reduce the thrust of supersonic nozzles. Maximum thrust can be achieved with a nozzle length that permits obtaining uniform flow at the exit. If the length limitation does not permit this, then the use of freedom in gas rotation might increase the nozzle thrust.

Dutton[17] investigated swirling flow in supersonic propulsion nozzles both numerically and experimentally. Computations were performed for a range of nozzle geometries, inlet swirl profiles, and swirl strengths. A time-dependent finite-difference technique was developed. The numerical results demonstrated, in agreement with the experimental data, that swirl has a minor effect on the specific impulse efficiency.

Knowles[18] examined the practical possibility of reducing shock-associated noise and controlling mass flow in a supersonic jet by means of swirl. It was found that nozzle performance does not degrade with the introduction of swirl; on the contrary, specific thrust can be increased with swirl. However, the swirl velocity profile needs to be carefully controlled. It was recommended that specific case studies be made to consider swirl in variable engine cycles.

Carpenter[19] developed a linearized theory for under-expanded inviscid supersonic jets with arbitrary initial swirl. Estimates were made of the effect of swirl on the total radiated sound power of shock-associated noise. It was found that this noise can be greatly reduced, or even eliminated, at sufficiently high swirl levels, which can be achieved at the expense of a very small thrust loss. Noise elimination was believed to be due to enhanced mixing that leads to the disappearance of some initial shock cells.

In another study more pertinent to mixing in free supersonic flows Yu et al.[20] experimentally examined mode-switching phenomena of supersonic jets with swirl. They observed that the shock-cell spacing of swirling jets is smaller than that of non-swirling ones, which suggests enhanced mixing. In non-swirling compressible jets, the typical two-dimensional vortex roll-up is believed to be suppressed, and mixing and entrainment are reduced, as compared to incompressible jets. Therefore, to counter the adverse effects of compressibility on mixing, adding swirl to a supersonic jet is favorable. The enhanced entrainment and mixing in swirling supersonic jets is thought to be due to the inherent three-dimensionality associated with the axial component of turbulent vorticity in swirling jets.

Yu[21] studied underexpanded supersonic jets to determine the effect of swirl on mixing efficiency. The screech tones, which result from the interaction of shock waves with unstable jet boundaries, were examined at different degrees of swirl for their effect on mixing. Implication of enhanced mixing was discussed. It was also reported that swirl did not eliminate shock cells, nor did it affect their quasi-periodic nature, despite the generation of a recirculation zone in strongly swirling jets.

Vortex enhancement of supersonic mixing was studied experimentally by Settles.[22] Swirl was utilized to enhance shear layer growth and mixing at high convective Mach numbers. It was concluded that swirl enhances compressible mixing; the degree of enhancement increases with increase in swirl strength. The effects of convective Mach number and density ratio on enhancement effect of swirl are still unknown and thus recommended for future work.

In an experimental investigation, which is very pertinent to this current study, Lee et al.[23] examined the near-field flow structure of underexpanded coaxial swirl jets. Swirl streams were issued from a secondary annular nozzle, while a primary inner nozzle provided the underexpanded free jets. The interactions between the annular swirl and the underexpanded core jets were examined, in order to quantify the effects of swirl stream on underexpanded jets. It was shown that the presence of an annular swirl stream causes the core-flow Mach disc to move further downstream, with an increased diameter.

In another pertinent study Lee et al.[24] investigated the effect of nozzle inlet configuration on under-expanded swirling jets, which were generated by a convergent nozzle with four tangential inlets at the supply chamber. The nozzle inlet configuration was modified by using different plugs, holes, and needles, which were also utilized as tools for measuring the flow properties at nozzle inlet. The experimental results showed that a needle inside the nozzle supply chamber can be used to control the under-expanded swirling jets. The structures of these jet flows are highly dependent on the detailed configuration of nozzle supply chamber.

Murakami and Papamoschou[25] examined flow structure and mixing enhancement in 2D and axisymmetric supersonic jets surrounded by secondary annular subsonic coaxial ones. The supersonic jets were issued from a convergent-divergent nozzle operated at off-design conditions. It was shown that the mixing enhancement using secondary parallel injection (referred to as MESPI by the researchers) halves the length of potential core in both round and 2D jets. A short distance past the potential core, mixing enhancement caused a reduction in centerline Mach number of 30% in round jets and 20% in 2D ones. The corresponding reduction in peak molar concentration of a scalar injected in the primary flow was 65% in round jets and around 40% in 2D ones.

The present work provides an experimental investigation of the effect of imparting swirl to underexpanded supersonic airflow on mixing. Such effect has not been fully quantified in the literature yet, due to the intrinsic three-dimensional nature of swirling supersonic flows. Non-reacting conditions are considered here, wherein inert gases are used to simulate gaseous fuel in underexpanded nozzle airflow. The focus is to quantify the effects of swirl, convective Mach number, and air-fuel density ratio on mixing.

II. Experimental Setup

This work complements the analysis of our experimental study[3] on the effects of swirl, convective Mach number, and air-fuel density ratio on shock structure in free under-expanded supersonic-nozzle airflows. The effects of the above parameters on mixing are investigated here. All the experiments have been performed on the UMD supersonic test facility shown here in Figure 3. A convergent nozzle of inlet-to-exit area ratio of 25 generates a free underexpanded supersonic airflow. At a reservoir pressure of about 7.8 atm (abs.) a near-field Mach number of 2.0 is achieved. The nozzle has swirling capabilities, wherein the axial-tangential-entry technique with four tangential inlets is utilized to accurately control the degree of swirl imparted to airflow. This technique has been proven in previous research to be an efficient method for generating supersonic swirling jets.[26]

A coaxial fuel-injection system injects fuel along the axis of air nozzle. The injection system can be positively and negatively recessed along the nozzle centerline to change the location of fuel injection with respect to airflow shock structure, if needed. A support flange upstream of nozzle ensures and maintains concentricity of the fuel injection system with respect to air nozzle, especially under swirling conditions. This flange comprises a conical sleeve that embraces injection system. The sleeve wall-thickness decreases in the direction of flow to provide streamlined performance and reduce blockage close to the nozzle exit. The sleeve is held in place by three spokes extending to the support flange. The spokes are distributed evenly at 120° along tangential direction. Their thickness has been optimized to provide rigidity with minimum blockage to incoming axial component of airflow. It should be noted here that those spokes are located physically upstream of air tangential inlets and do not affect the flowfield of tangential air component. Some wakes are expected to exist in axial-component flowfield behind the spokes, but the supersonic flow exiting the nozzle was found to be fully axisymmetric in the presence as well as absence of tangential component.

The experimental results presented in this study have been obtained using a novel nanosecond condensate-seeded Mie-scattering diagnostic technique. The airflow is saturated with diethyl-ether (C_2H_5-O-C_2H_5) vapor upstream of the nozzle. As airflow temperature decreases during expansion, diethyl-ether condensates back to form submicron ($\approx 0.5\ \mu m$) seed particles that are small enough to follow the flow faithfully. A stream of liquid diethyl-ether is solid-atomized through a 0.020-in orifice, and the resulting droplet jet is injected into high-pressure airflow way upstream of nozzle. The droplets evaporate rapidly, and the vapor mixes thoroughly with air saturating it. A controlled flow rate is injected, in order to provide adequate visualization of flowfield while preventing over-saturation of airflow, which can result in the formation of a liquid diethyl-ether film on the internal walls of nozzle or air delivery system. Diethyl-ether was chosen as the

visualization medium, because it has the unique property of being highly volatile at atmospheric conditions. A boiling point of ~35 °C allows diethyl-ether to evaporate easily into the 300-K incoming airflow and then condense back easily as air cools during expansion. Moreover, a freezing point of −116 °C prevents diethyl-ether from freezing in the cold supersonic airflow. A schematic of the Mie-scattering setup is shown in Figure 4.

The supersonic flowfield is illuminated by means of a 6-ns pulse Nd:YAG laser sheet along a centerline plane. The Mie-scattering signal is captured using a 5-ns gated Princeton Instruments PI-MAX2:1003 UNIGEN2 digital ICCD camera operated in synchronization with the laser. Such nanosecond duration prevents the seeding particles from creating light streaks on the captured images. A resolution of 1024 x 1024 pixels was set for all images presented here. The intensity distribution of Mie-scattering signal is used to highlight mixedness distribution, shock structure, shear layers, and slip lines within flowfield.

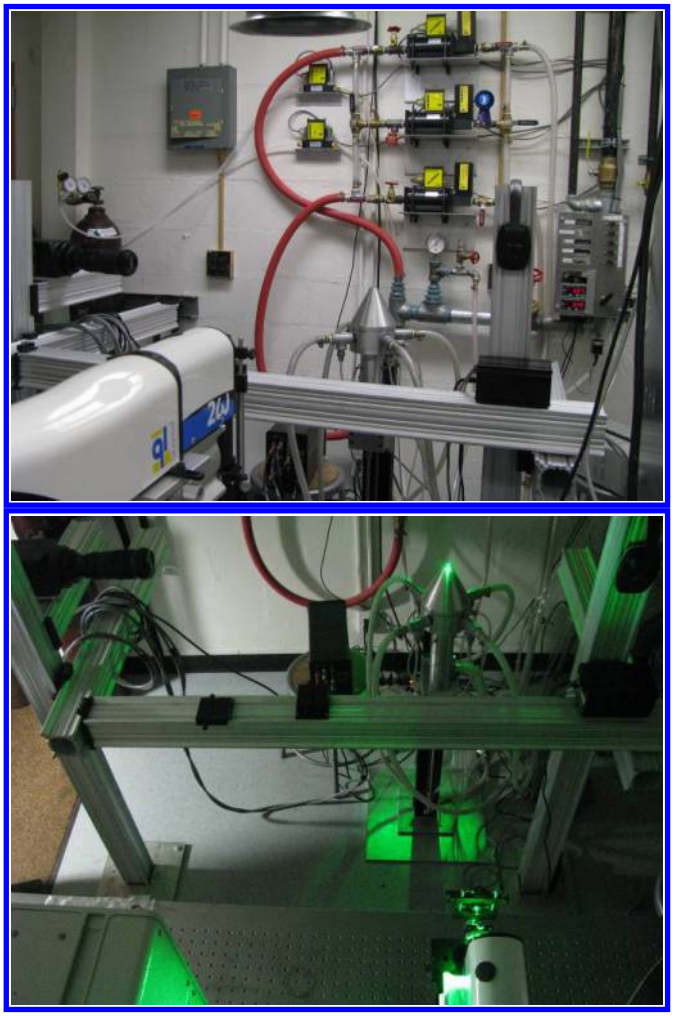

Figure 3. Supersonic facility at UMD Combustion Laboratory

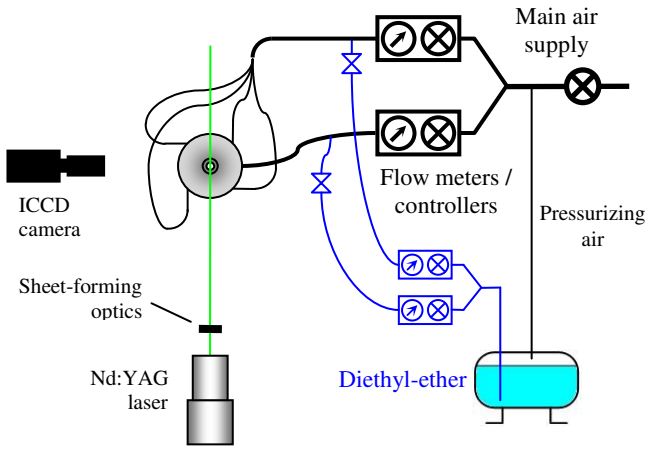

Figure 4. Schematic of the utilized Mie-scattering setup

III. Test Matrix

Table 1 lists the test matrix for the results presented here. The effects of M_{conv} and DR are investigated, both under non-swirling as well as swirling conditions. Following the approach of Abdelhafez and Gupta,[3] M_{conv} is defined here as:

$$M_{conv} = \frac{v_{air} - v_{fuel}}{a_{air}} = M_{air} - \frac{v_{fuel}}{a_{air}}$$

This definition relates the velocity difference between fuel and air to the speed of sound in air. It should be noted that the fuel stimulant is injected here at velocities smaller than those of supersonic airflow. Therefore, the injectant velocity is subtracted from air velocity in this definition of M_{conv}, in contrast to the common definition given in literature.

Since the investigated underexpanded airflow undergoes expansion after exiting nozzle, the near-field Mach number is not constant. Nevertheless, the maximum value will be used in our definition of M_{conv} above. The shock structure and all properties of airflow, including M_{air}, depend on air total pressure and temperature. Both were kept constant at 7.9 bar (abs) and 300 K, respectively, for all cases presented in this study. Based on isentropic ideal-gas relations, the corresponding maximum value of M_{air} equals 2.0. This value is concurred by the area-Mach-number relationship, which confirms a Mach number of 2.0 at the maximum flow cross-sectional area downstream of nozzle exit. Further details on shock structure are given in next section.

Non-reacting conditions are considered in this present work, wherein gaseous fuel is simulated by inert gases (helium, and argon). At constant airflow properties, helium was injected at different flow rates to induce various helium velocities and thus multiple values of M_{conv}. The effect of DR is also examined at constant airflow properties. Different mixtures of inert gases simulate fuel; mixture composition

was changed from one case to the other to induce different mixture densities and thus multiple DR. The flow rate of inert-gas mixture was adjusted to adapt for its changing density and maintain a constant velocity, which resulted in constant M_{conv}. Analyses of the effects of swirl, M_{conv}, and DR on mixing were made.

A total of 20 cases are presented here (10 non-swirling cases and their swirling counterparts). Due to the intrinsic three-dimensionality of swirling flows, no simple calculations of M_{air} could be carried out for the swirling cases. The nominal non-swirling maximum value of 2.0 was used instead. Five case-pairs study the effect of M_{conv}, wherein the injectant (helium) velocity was changed. The effect of DR is studied through four pairs, where the injectant comprises different inert-gas mixtures. The mixture composition governs its density and consequently DR. Note that a letter "s" next to a case number in Table 1 denotes a swirling case.

Following a definition used for incompressible swirling jets,[27,28] a geometrical swirl number S_g is defined for air as

$$S_g = \left(\frac{\pi r_o R_o}{A_t} \right) \frac{m_t}{m_a + m_t}$$

where $(\pi r_o R_o / A_t)$ = 0.68, for the geometry of the UMD nozzle and its tangential entries. (m_a) and (m_t) are the axial and tangential components of airflow, respectively. These flow rates were controlled and measured using thermal flow controllers/meters of ±1.5% full-scale accuracy.

Table 1. Test Matrix

Nozzle reservoir pressure = 7.9 bar, abs. (constant)
Air total temperature at inlet = 300 K (constant)
Geometrical swirl number (swirling cases), S_g = 0.68 (const.)

Case	Injected Gas	M_{conv}	DR
0 & 0s	Air only, no fuel injection		
Effect of Convective Mach Number			
1 & 1s	Helium	1.91	36.73
2 & 2s		1.81	
3 & 3s		1.72	
4 & 4s		1.63	
5 & 5s		1.53	
Effect of Density Ratio			
6 & 6s	80% Helium / 20% Argon	1.42	13.12
7 & 7s	60% Helium / 40% Argon		7.98
8 & 8s	40% Helium / 60% Argon		5.74
9 & 9s	20% Helium / 80% Argon		4.48

IV. Results and Discussion

Shock Structure (Non-Swirling, No Injection System)

The shock structure of simple underexpanded supersonic flow is shown schematically in Figure 5. A shock-cell unit gets repeated periodically to form the shock-cell train. This unit can be described as follows. Axial under-expanded flow undergoes an expansion fan and turns outwards. The free-jet boundary adapts accordingly and turns outwards as well. Passing again through the expansion fan, the outward flow turns back to axial. As the expansion fan meets the boundary, it reflects into a compression fan that coalesces later into the intercepting shock wave. The annular flow adjacent to boundary turns inwards through the compression fan, and the boundary again adapts by turning inwards as well. For slightly underexpanded nozzles, this intercepting shock reflects directly into a reflected shock at the centerline, forming the familiar diamond configuration. However, as the pressure ratio across the nozzle is increased, this reflection no more takes place at the centerline, and a Mach disk (normal shock) is formed. The reflected shock turns the inward annular flow back to the axial direction. Since the Mach disk decelerates core flow to subsonic speeds, a slip line originates from the origin of reflected shock to separate the subsonic core flow from the supersonic annular one. As the reflected shock impinges on outer free flow boundaries, it reflects into an expansion fan, starting another shock-cell unit. The repetition of units continues until viscous effects dominate the flow, and this structure is no longer observed.

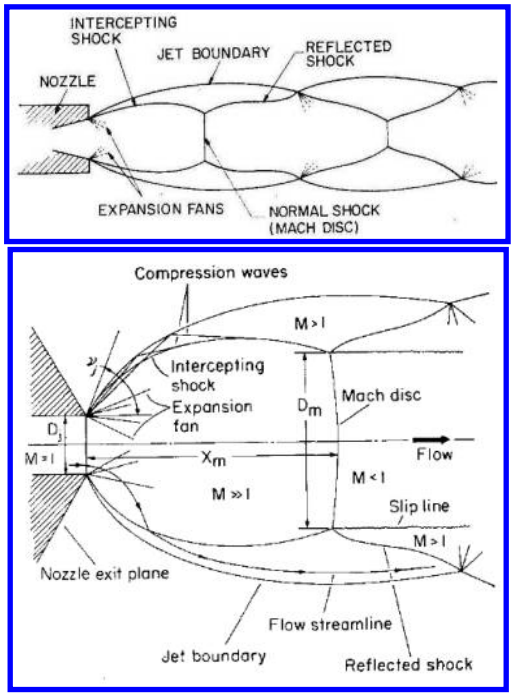

Figure 5. Schematic of shock structure of simple highly under-expanded nozzle flow. Top: Adamson and Nicholls [10]; Bottom: Crist et, al. [11]

In presence of a coaxial injection system, the shock structure differs significantly from the simple one described above. Figure 6 shows Schlieren[3] and Mie-scattering images of the shock structure of underexpanded nozzle flow in the presence of a non-recessed coaxial injection system with no fuel injection. Two distinct sub-structures are identifiable; the simple nozzle-rim structure discussed above and a new one generated due to the existence of coaxial injection system. In this study from here onwards, the nozzle-rim and injection-system sub-structures will be denoted "primary" and "secondary" shock structures, respectively.

The secondary structure starts with the airflow generating inner conical boundaries that complete the cone-frustum shape of fuel system tip.[3] The flow collapses into itself at the centerline, generating a conical shock wave that turns the flow back to parallel. This shock wave impinges on the outer flow boundaries shortly downstream of the impingement location of nozzle-rim expansion fan. The outer boundaries are altered by the impingement of that conical shock as observed from Figure 6. The shock reflects into an expansion fan that creates its own compression fan, intercepting shock, Mach disk, and reflected shock, similar to the primary structure. Both Mach disks of primary and secondary structures appear distinctly in Figure 6.

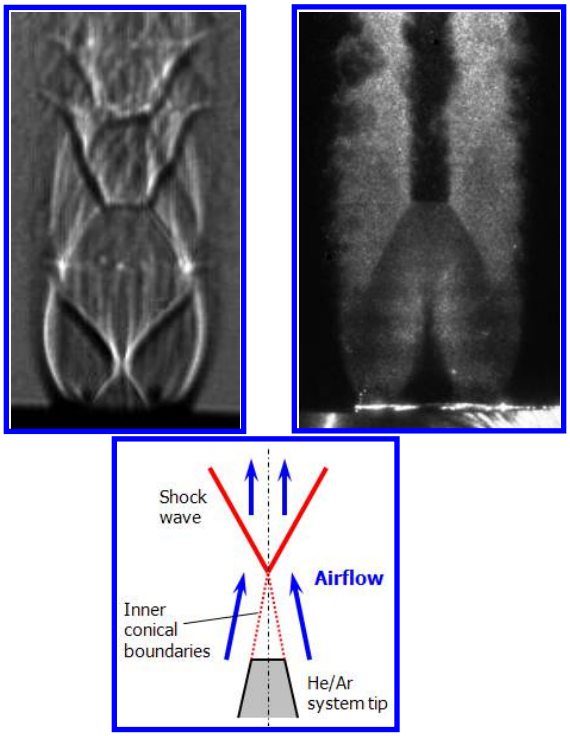

Figure 6. Images of free non-swirling underexpanded nozzle airflow in presence of non-recessed coaxial injection system with no fuel injection. Top left: Schlieren image from Abdelhafez and Gupta [3]; Top right: Mie-scattering image (present study); Bottom: Schematic of shock structure of core flow from Abdelhafez and Gupta [3]

Several important observations can be made from the Mie-scattering image in Figure 6. The first observation is the existence of a dark conical core region downstream of nozzle exit. This region is bounded by the inner conical boundaries described earlier. Almost no diethyl-ether seeding particles exist within that region, hence its dark appearance. The conical shock wave of secondary structure is identifiable downstream of the dark region. All other major shocks of flowfield are identifiable as well, such as intercepting shock, Mach disk, and reflected shock. The second important observation to be made here is that the intensity of Mie-scattered light increases after the flow passes through each shock. This is attributed to flow compression. The dense fog of seeding particles downstream of a shock wave scatters more light. Based on this observation it can be concluded which shocks are stronger than others. The intercepting shock, for example, is distinctly stronger than the reflected one. The Mach disk is an exception of this rule. Being a normal shock, it decelerates core flow to subsonic speeds, raising its temperature significantly. The higher temperature is believed to cause evaporation of the diethyl-ether liquid seeding particles. This explains the dark appearance of subsonic core flow downstream of Mach disk between the slip lines, since the seeding particles exist no more.

Imparting Swirl to Airflow (No Fuel Injection)

The effect of swirl is investigated here by introducing entire airflow through nozzle tangential inlets. Based on aforementioned definition, the resulting geometrical swirl number should be 0.68 in the absence of coaxial injection system. However, since the current geometry involves one, the effect of injection-system presence is to reduce the sonic swirl number to 0.36 only at nozzle throat. The reader is referred to the numerical study of Abdelhafez and Gupta[29] for more details on the variation of swirl number within flowfield.

Figure 7 highlights the effect of swirl by comparing the non-swirling and swirling flowfields of cases 0 and 0s from Table 1. The corresponding Schlieren images from the work of Abdelhafez and Gupta[3] are shown on the top row followed by the Mie-scattering images of current study. The most remarkable observation to be made from the Mie-scattering images is that swirl enhances mixing significantly, which agrees with the findings of most studies in the aforementioned literature review. The added streamwise vorticity alleviates the negative effect of gas compressibility. A clear example is evident in the smeared slip lines and narrower subsonic core downstream of first shock cup in the swirling flowfield. Enhanced mixing occurs between the supersonic and subsonic sides of slip lines, which is absent across the sharp slip lines of non-swirling flowfield. Another important finding of Figure 7 is that swirl reduces the strength of shock structure, which was concluded from the analysis of Schlieren images as well. From the Mie-scattering point of view, weaker shocks are evidenced by

smaller differences in the intensities of scattered light before and after each shock. For example, the intercepting shock undergoes greater reduction in strength as compared to the other shocks. The third and final observation to be made from Figure 7 is that the dark conical region downstream of nozzle exit shrinks with the application of swirl. It was explained in the analysis of Schlieren images that the greater dark region identifiable downstream of nozzle exit in the Schlieren image of swirling flowfield is a greater nozzle-rim expansion fan that overtakes the inner conical boundaries at tip of secondary shock structure, which results in reduction of the shock strength. This finding is concurred by the Mie-scattering image of swirling flowfield, where the inner conical boundaries are smeared and the dark conical region is clearly of a smaller size, which is attributed to a greater nozzle-rim expansion fan.

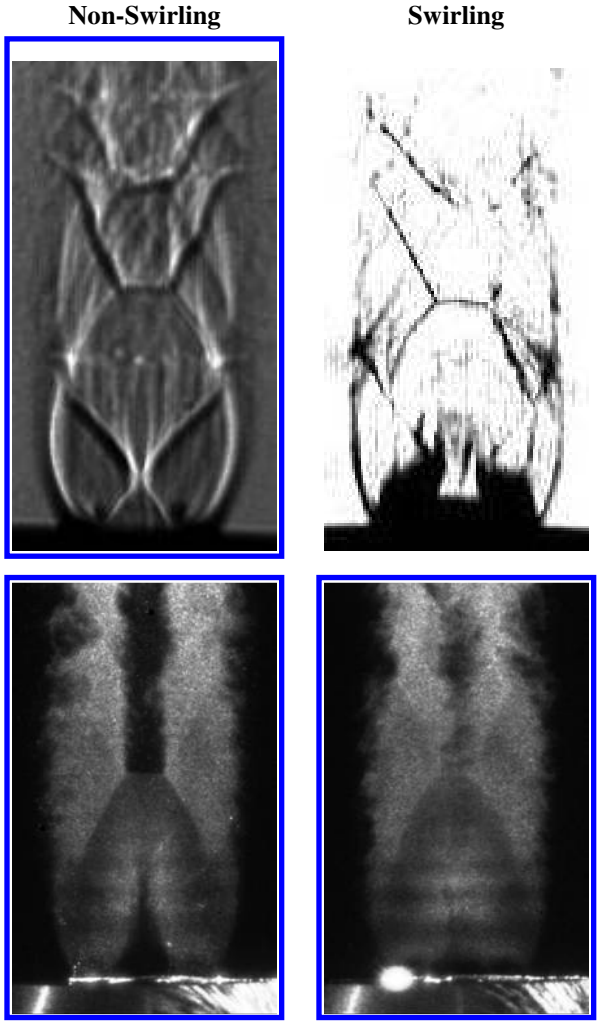

Figure 7. Images of non-swirling (left) and swirling (right) underexpanded nozzle airflow with no fuel injection. Top: Schlieren images from Abdelhafez and Gupta [3]; Bottom: Mie-scattering images (current study)

Effect of Convective Mach Number (M_{conv})

The effect of M_{conv} is examined in case-pairs 1 – 5 given in Table 1. Keeping all air properties constant, the flow rate of fuel (helium) was changed to induce different helium velocities and thus multiple values of M_{conv}, based on the aforementioned discussion. The injection Mach number of helium was kept below 0.3 to avoid compressibility effects on the helium-side of air/helium shear layer and to maintain a constant helium density. This resulted in a DR of 36.73 for all five case-pairs. The supply pressure of helium was carefully selected for each case-pair to have an injection pressure matching the throat pressure of airflow.

Figure 8 shows Mie-scattering images of case-pairs 1 – 5. Non-swirling cases are depicted in the top row, while the bottom one contains swirling cases. The values of M_{conv} and helium injection Mach number of each case-pair are indicated at the top of its column. Incompressible injection is implemented in all case-pairs with $M_{He} \leq 0.3$. It should be noted that the speed of sound in helium is about three times that of air (at 300 K). Therefore, an injection velocity of 150 m/s corresponds to an incompressible helium Mach number of about 0.15 but a compressible 0.43 Mach number in air.

The most remarkable conclusion to be made from Figure 8 is that the compressibility of helium jet significantly affects the shape of air/helium shear layer within the first nozzle-exit diameter downstream of throat. The incompressible helium jets are observed to have a converging cross-sectional area, i.e., negative shear angle, up to z/D of about 0.5. Afterwards, the shear angle transitions to positive. Incompressible helium jets have low densities, allowing for easy expansion of the denser airflow radially inwards, which explains the negative shear angles. After considerable mixing with airflow the density of mixed core jet becomes high enough to allow for a positive-shear-angle propagation. This behavior has been reported in the numerical study of Abdelhafez and Gupta.[29] It was demonstrated over an extended range of M_{conv} that compressible injection results in earlier transition to the positive-shear-angle propagation. At injection Mach numbers as high as 0.6 the helium jet was shown to propagate with a positive shear angle almost from the start.

Another observation to be deduced from Figure 8 is that decreasing M_{conv} results in a stronger shock structure, which is evidenced in greater differences in intensities of scattered light before and after each shock. The intercepting shock is again the clearest example. This trend is also in agreement with the findings of our previous studies.[3,29] Negative initial shear angles allow for the development of a compression fan on the air side of curved shear layer. This fan later coalesces into a shock wave that creates the secondary shock structure. At low M_{conv} this compression fan is replaced by a single oblique shock. The gradual near-isentropic compression through compression fan results in a weaker shock structure, even if that fan later coalesces into a shock itself. Therefore, low-M_{conv} flowfields have stronger shock structures.

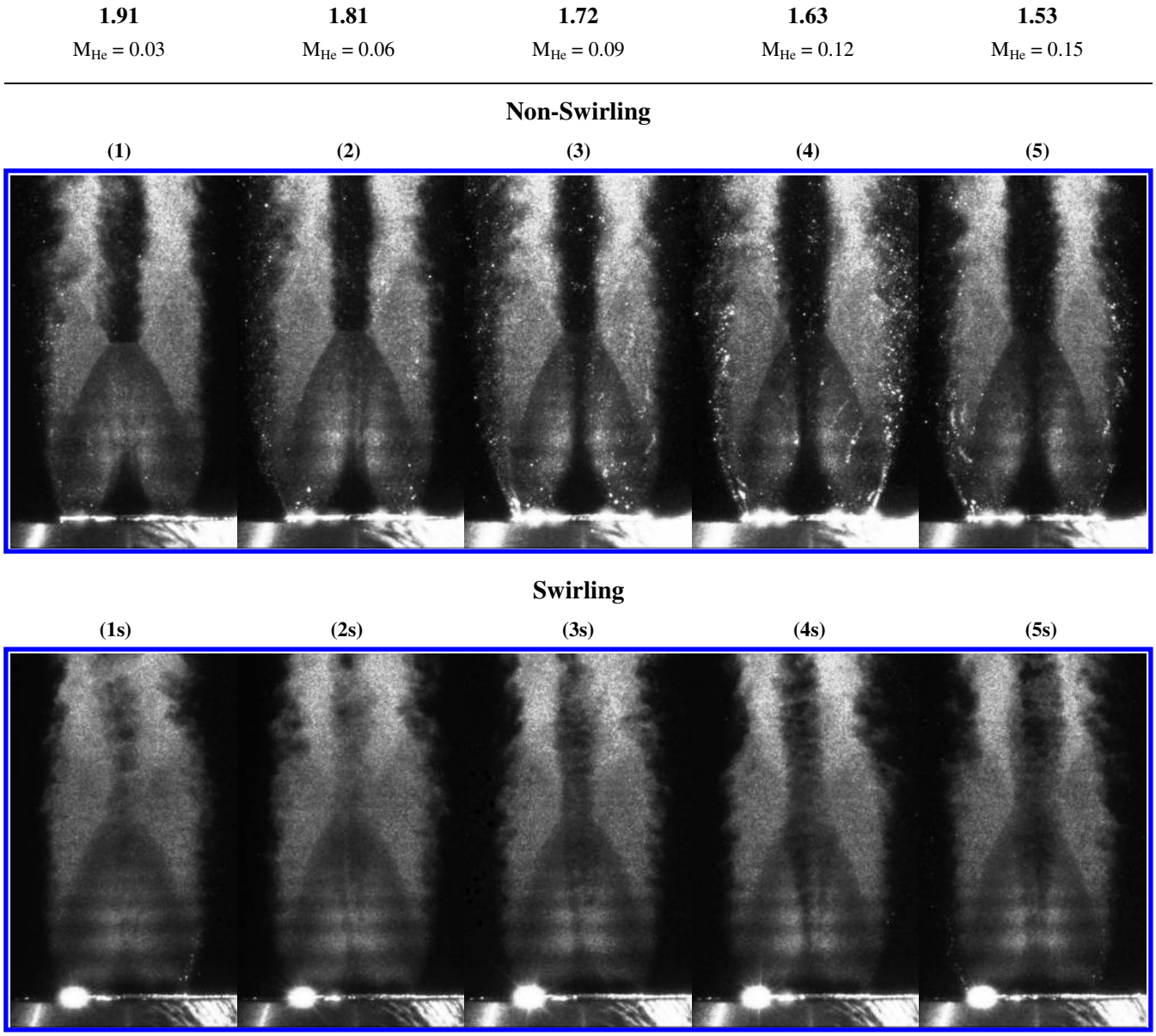

Figure 8. Effect of M_{conv}; DR = 36.73

A third observation to be inferred from Figure 8 is that the low helium flow rate and injection Mach number, characteristic of high M_{conv} such as 1.91 in case-pair 1, allow for near-complete mixing of helium jet with the surrounding airflow. The extended dark core region, representative of high helium concentrations upstream of first primary Mach disk, is almost absent, which indicates that the interactions of shock structure with air/helium shear layer are sufficient to achieve complete mixing. This behavior disappears steadily as M_{conv} is reduced, which is expected for higher helium flow rates. Moreover, it can be observed that mixing is poorer within second shock cell as compared to the first. This is evidenced in the significant difference in light intensity between the supersonic annular flow and the subsonic core one downstream of first primary Mach disk. Compared to the first shock cell, the second one has weaker shock waves and a high-density compressible core flow. The effects of the decreasing density gradient across slip line and the smaller pressure gradients across shocks add up to yield a weaker and less effective Baroclinic vorticity vector, which explains the deteriorated mixing.

If the non-swirling cases are to be finally compared to their swirling counterparts, the same aforementioned findings can be made. Imparting swirl to airflow results in significant mixing enhancement, which is evidenced in the lighter shades of core helium flow in all swirling cases. Some reduction in strength of shock structure is also observed.

Effect of Air-Fuel Density Ratio (DR)

The effect of DR is examined in case-pairs 6 – 9 given in Table 1. Different mixtures of inert gases (helium and argon) simulate fuel; mixture composition was changed from one case-pair to the other to induce different mixture densities and thus multiple values of DR. The flow rate of inert-gas mixture was adjusted to adapt for its variable density and maintain a constant velocity, which resulted in a constant M_{conv} of 1.42. The supply pressure of fuel simulant was carefully selected for each case-pair to have an injection pressure matching the throat pressure of airflow.

Figure 9 shows Mie-scattering images of case-pairs 6 – 9. Note that the non-swirling cases are depicted in the top row, while the bottom one contains swirling cases. The values of DR and fuel injection Mach number of each case-pair are indicated at the top of its column together with the composition of utilized fuel simulant. Compressible injection is implemented in all case-pairs. Lower levels of mixedness are detected in Figure 9, as compared to the ones observed earlier in analysis of M_{conv}. The lack of good mixedness here can be explained by the higher densities of fuel jets, which result in smaller density gradients across air/fuel shear layer and consequently weaker Baroclinic vorticity vectors.

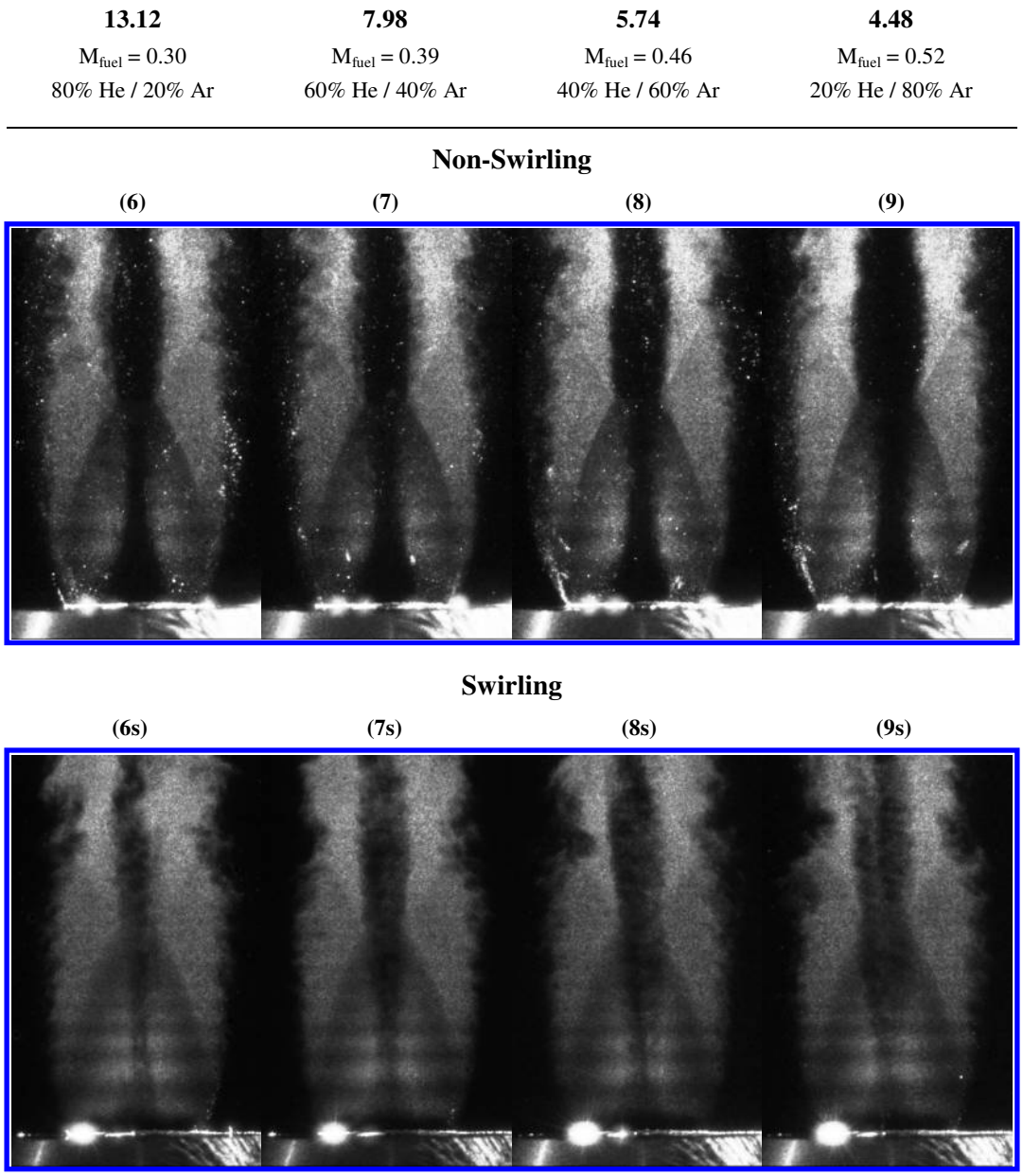

Figure 9. Effect of DR; M_{conv} = 1.42

Smaller negative initial air/fuel shear angles are observed that transition to positive after shorter axial distances of jet travel. This behavior favors the direct formation of an oblique shock wave, rather than a compression fan, at the origin of secondary shock structure. Therefore, the shock structures of case-pairs 6 – 9 are on the average stronger than those of case-pairs 1 – 5 studied earlier. The advantageous shock-induced mixing enhancement is, however, overcome by the stronger negative effect of fuel-jet compressibility.

A comparison of non-swirling cases to their swirling counterparts reveals once more that imparting swirl to airflow results in significant mixing enhancement, which is again evidenced in the lighter shades and smaller widths of core helium flows in all swirling cases. Some reduction in strength of shock structure is also observed.

V. Conclusions

The effects of swirl, convective Mach number, and air-fuel density ratio have been investigated experimentally in free underexpanded nozzle airflow with subsonic non-recessed coaxial fuel injection. A nanosecond condensate-seeded Mie-scattering diagnostic technique was used to highlight the effects of those parameters on mixing. The following conclusions can be made. (a) The presence of non-recessed coaxial fuel-injection system results in the formation of an additional shock sub-structure within airflow. In addition to the simple nozzle-rim structure, a new one is generated due to the existence of injection system. (b) Swirl enhances mixing significantly. The added streamwise vorticity alleviates the negative effect of gas compressibility. (c) Swirl reduces the strength of shock structure, which agrees with the findings of our previous studies. The application of swirl results in a greater nozzle-rim expansion fan that overtakes the inner conical boundaries at tip of secondary shock structure, thus resulting in reduction in shock strength. (d) Higher convective Mach numbers allow for near-complete mixing of fuel jet with the surrounding airflow, as the interactions of shock structure with air/helium shear layer are sufficient to achieve complete mixing. This behavior disappears steadily as convective Mach number is reduced. (e) The shear angle between fuel and air jets depends on fuel compressibility and air-fuel density ratio. Incompressible fuel jets and/or high air-fuel density ratios result in negative shear angles, which transition to positive if the fuel jet becomes compressible or the density gradient across shear layer decreases. (f) Negative shear angles induce weaker shock structures. Shock strength increases as shear angle transitions to positive. (g) If the densities of fuel and air jets are comparable, smaller density gradients exist across air/fuel shear layer, which translates into weaker Baroclinic vorticity vector and consequently deteriorated mixedness.

Acknowledgments

This work was supported by the Space Vehicle Technology Institute under grant NCC3-989, jointly funded by NASA, DoD, and USAF within NASA Constellation University Institutes Project (CUIP), with Claudia Meyer as the Project Manager. This support is gratefully acknowledged.

The valuable suggestions of Dr. Kenneth Yu during design and development of Mie-scattering system are gratefully acknowledged.

References

[1]Gruber, M.R., Nejad, A.S., Chen, T.H., and Dutton, J.C., "Mixing and Penetration Studies of Sonic Jets in a Mach 2 Freestream," Journal of Propulsion and Power, Vol. 11, No. 2, March-April 1995.

[2]Kutschenreuter, P., "Supersonic Flow Combustors," Scramjet Propulsion, Progress in Astronautics and Aeronautics Series, Vol. 189, 2000, pp. 513 – 567.

[3]Abdelhafez, A. and Gupta, A. K., "Swirl Effects on Shock Structure in Free Under-expanded Supersonic-Nozzle Airflow," 44th AIAA/ASME/SAE/ASEE Joint Propulsion Conference & Exhibit, Hartford, CT, July 21-23, 2008, AIAA-2008-4502.

[4]Sung, C. J., Li, J. G., Yu, G., and Law, C. K., "Chemical Kinetics and Self-Ignition in a Model Supersonic Hydrogen–Air Combustor," AIAA Journal, Vol. 37, No. 2, February, 1999, pp. 208-214.

[5]Conaire, M. O., Curran, H. J., Simmie, J. M., Pitz, W. J., and Westbrook, C. K., "A Comprehensive Modeling Study of Hydrogen Oxidation," International Journal of Chemical Kinetics, Vol. 36, No. 11, pp. 603-622.

[6]Ben-Yakar, A., "Experimental Investigation of Transverse Jets in Supersonic Cross-flows," Ph.D. Dissertation, Dept. of Mechanical Eng., Stanford Univ., Stanford, CA, Dec. 2000.

[7]Huh, H., and Driscoll, J. F., "Measured Effects of Shock Waves on Supersonic Hydrogen-Air Flames," 32nd Joint Propulsion Conference and Exhibit, Lake Buena Vista, FL, July, 1996, AIAA-96-3035.

[8]Yang, J., Kubota, T., and Zukoski, E. E., "Applications of Shock-Induced Mixing to Supersonic Combustion," AIAA Journal, Vol. 31, No. 5, May 1993, pp. 854 – 862.

[9]Menon, S., "Shock-wave-induced mixing enhancement in scramjet combustors," 27th AIAA Aerospace Sciences Meeting, Reno, NV, Jan 1989, AIAA-89-0104.

[10]Adamson, T. C., Jr. and Nicholls, J. A., "On the Structure of Jets from Highly Underexpanded Nozzles into Still Air," Journal of the Aero/Space Sciences, Vol. 26, No. 1, January, 1959, pp. 16-24.

[11]Crist, S., Sherman, P. M., and Glass, D. R., "Study of the Highly Underexpanded Sonic Jet," AIAA Journal, Vol. 4, No. 1, 1966, pp. 68-71.

[12]Lewis, C. H., Jr. and Carlson, D. J., "Normal Shock Location in Underexpanded Gas and Gas-Particle Jets," Technical Note, AIAA Journal, Vol. 2, No. 4, April, 1964, pp. 776-777.

[13]Gostintsev, Y. A., Zelentsov, V. V., Ilyukhin, V. S., and Pokhil, P. F., "Structure of Underexpanded Supersonic Swirling Gas Jet,"

Journal of Fluid Dynamics, Vol. 4, No. 5, September, 1969, pp. 158-162.

[14]Lewellen, W. S., Burns, W. J., and Strickland, H. J., "Transonic Swirling Flow," AIAA Journal, Vol. 7, No. 7, July, 1969, pp. 1290-1297.

[15]Batson, J. L. and Sforzini, R. H., "Swirling Flow through a Nozzle," Journal of Spacecraft and Rockets, Vol. 7, No. 2, February, 1970, pp. 159-163.

[16]Naumova, I. N. and Shmyglevskii, Y. D., "Nozzle Thrust Increase by Flow Rotation," Journal of Fluid Dynamics, Vol. 2, No. 1, January, 1967, pp. 23-25.

[17]Dutton, J. C., "Swirling Supersonic Nozzle Flow," Journal of Propulsion and Power, Vol. 3, No. 4, 1987, pp. 342-349.

[18]Knowles, K., "Combined Noise and Flow Control of Supersonic Jets Using Swirl," 14th DGLR/AIAA Aeroacoustics Conference, Aachen, Germany, May 11-14, 1992.

[19]Carpenter, P. W., "A Linearized Theory for Swirling Supersonic Jets and Its Application to Shock-Cell Noise," AIAA Journal, Vol. 23, No. 12, 1985, pp. 1902-1909.

[20]Yu, Y. K., Chen, R. H., and Chew, L., "Screech Tone Noise and Mode Switching in Supersonic Swirling Jets," AIAA Journal, Vol. 36, No. 11, pp. 1968-1974.

[21]Yu, Y. K., "An Experimental Study of Underexpanded Supersonic Swirling Jets," PhD thesis, University of Central Florida, December 1997.

[22]Settles, G. S., "Supersonic Mixing Enhancement by Vorticity for High-Speed Propulsion," Report submitted to NASA-Langley Research Center, October 1991, NASA-CR-188920.

[23]Lee, K. H., Setoguchi, T., Matsuo, S., and Kim, H. D., "An Experimental Study of Underexpanded Sonic, Coaxial, Swirl Jets," Proceedings of the Institution of Mechanical Engineers, Part C: Journal of Mechanical Engineering Science, Vol. 218, No. 1, 2004, pp. 93-103.

[24]Lee, K. H., Setoguchi, T., Matsuo, S., and Kim, H. D., "Influence of the Nozzle Inlet Configuration on Under-Expanded Swirling Jet," Proceedings of the Institution of Mechanical Engineers, Part C: Journal of Mechanical Engineering Science, Vol. 220, No. 2, 2006, pp. 155-163.

[25]Murakami, E. and Papamoschou, D., "Experiments on Mixing Enhancement in Dual-Stream Jets," 39th AIAA Aerospace Sciences Meeting & Exhibit, Reno, NV, Jan 8-11, 2001, AIAA-2001-0668.

[26]Cutler, A. D., Levey, B. S., and Kraus, D. K., "Near-Field Flow of Supersonic Swirling Jets," AIAA Journal, Vol. 33, No. 5, May 1995, pp. 876-881.

[27]Gupta, A. K., Lilley, D. G., and Syred, N., "Swirl Flows," Abacus Press, UK, 1984, ISBN 0-85626-175-0.

[28]Claypole, T. C. and Syred, N., "The Effects of Swirl Burner Aerodynamics on NOx Formation," Proceedings of 18th Symposium (International) on Combustion, Combustion Institute, Pittsburgh, PA, 1981, pp. 81-89.

[29]Abdelhafez, A. and Gupta, A. K., "Swirl Effects on Mixing in Free Under-Expanded Supersonic-Nozzle Airflow," 47th AIAA Aerospace Sciences Meeting, Orlando, FL, Jan. 5-8, 2009, AIAA-2009-1419.